J Therm Anal Calorim (2012) 110:897–905
DOI 10.1007/s10973-011-1792-2

Heat transfer through fibrous assemblies by fractal method

W. F. Song · W. D. Yu

Received: 17 June 2011 / Accepted: 6 July 2011 / Published online: 7 October 2011

Abstract Fractal theory has been proved effective to characterize the complex pore structure. In this article, the fractal method is utilized to study the structure property of fibrous assemblies. The box dimension parameter is applied to characterize the pore structure of fibrous assemblies by analyzing the electronic scanning microscope images of the fibrous assemblies. Furthermore, a fractal model for predicting effective heat conductivity is established. Experiment is conducted to verify the model, and good agreement is found between the experimental and theoretical results. The fractal model is also compared with the previous models for predicating heat conductivity, and the former is proved to be more accurate.

Keywords Heat transfer · Fibrous assembly · Fractal method

Introduction

The effective heat conductivities of fibrous assemblies have received continuous attention [1–7] due to their various applications in clothing and engineering. The property, reported in several literatures, depends on the nature of pore size and distribution in a fibrous assembly [8–10]. Therefore, describing the pore structure properties of fibrous assemblies is of great importance. Several researches have discovered the fractal features of porous media [11–14]. As is known, the fibrous assembly is a kind of porous media, consisting of fibers and air, and the fractal method is also feasible to investigate the pore structure of fibrous assemblies, which is found in a few papers [15–17]. In this article, we will also utilize the fractal method to study the pore nature of fibrous assemblies investigated here.

Numerous researchers have worked on the analytical calculation of the heat conductivity of fibrous assemblies [18–29]. Schuhmeister [18] was the first to develop a model for heat conductivity of fibrous structures that combines a parallel and series mode of heat transfer through the air and fiber phase. The model was utilized by many researchers for heat transfer study [1, 19]. In order to model the solid heat conduction through fibers and contact points, Hager and Steere [20] developed an empirical formula for calculating heat conductivity by combination of solid conduction with a series of thermal network for gas/solid conduction. Woo et al. [4] presented a more complicated heat transfer model of fibrous assemblies by considering fiber orientation and anisotropy, and the model is proved to be more accurate. However, the model contains so many parameters, which are complex to get. In the above models, heat transfer by radiation is not considered which are proved to take a large proportion in fibrous assemblies with high porosity or under high temperature [21–24]. Farnworth developed the two-flux model for studying heat transfer property of fibrous assemblies [25], and the model is widely used by later researchers for calculating combined heat and mass transfer properties [26, 27]. Veiseh et al. [28] proposed an empirical formula for fibrous assemblies by combining Langlais and Klarsfeld semi-empirical relation for conduction heat transfer and Larkin formula for radiation part, and the model is verified by fitting amount of experimental data. The above

W. F. Song · W. D. Yu
Textile Materials and Technology Laboratory, Donghua University, Shanghai 201620, People's Republic of China

W. F. Song · W. D. Yu (✉)
College of Garment & Art Design, Jiaxing University, Jiaxing 314001, Zhejiang, People's Republic of China
e-mail: wdyu@dhu.edu.cn

approaches, called "average volume" methods, are all based on the assumption that the fibrous assemblies are continuous medium, which makes it difficult to consider the influence of microstructures of pores, and thus the application of these existing porous media theories has some fundamental limitations.

Fractal theory has been applied to study permeability [11, 29, 30] and thermal conductivity of porous media [13, 31, 32]. Chen et al. [31] developed a fractal model to study effective heat conductivity of soil. Later, Yu et al. [32] proposed fractal models to calculate the effective thermal conductivity of mono- and bi-dispersed porous media, such as sandstone, particles, etc. The effective heat conductivity of wood [33], foam [34], and other objects were also discussed by some researchers [35, 36]. The above models established were based on the assumption that the objects investigated are exactly self-similar, which is not in accordance with real porous media. For real porous media, the microstructure such as pore sizes and particles are statistically self-similar. Kou et al. [37] investigated the effective heat conductivity of fibrous materials under this condition. The model assumed that the air and fibers are in parallel arrangement in the fibrous materials, which neglects the fiber-to-fiber contact effect on effective heat conductivity. The previous models also did not take radiative heat conductivity into consideration.

In this article, we will use fractal theory to study the structure of fibrous assemblies. A more complete fractal model for predicating effective heat conductivity of fibrous assemblies is established. Fiber-to-fiber contact influence to the effective heat conductivity was considered. Radiative heat conductivity was also taken into consideration. Experiment is conducted to verify the model. Parameter influence on effective heat conductivity is systematically discussed.

Experimental

Materials and testing device

A variety of nonwoven fabrics, one form of fibrous assembly, were selected for the samples. The specifications of these samples are listed in Table 1. The thickness was measured in accordance with ISO 5084-1996. The pressing pressure is 100 cN and the pressing time is 10 s. The area density was calculated by measuring the weight of a sample with the diameter of 10 cm using an electronical balance with the precision of 0.00001 g. The porosity of the samples is calculated by the following equation:

$$\varepsilon = 1 - \frac{\mu}{1000 L_0 \rho_f}, \tag{1}$$

where μ is the area density, L_0 is the thickness, and ρ_f is the fiber density.

The effective heat conductivity was measured by the Kawabata Thermolabo, which is in accordance to the Chinese National Standard GB11048-89. The temperature difference (ΔT) between the two sides of a sample is fixed during the testing and is set to be 10 °C here. The pressure applied to the sample is controlled to be 6 g/cm^2 here. According to Fourier law, when heat flux through materials (q) is stabilized, the heat conductivity k_{exp} can be expressed as:

$$k_{exp} = \frac{qL_0}{A\Delta T}. \tag{2}$$

Theory

Microstructure and fractal description of fibrous assemblies

As is known, an object measurement is related to its dimension and is invariant with the unit of measurement used. In general, ordered objects such as points, lines,

Table 1 Parameters of the nonwoven fabrics chosen

Sample number	Fiber type	Fiber diameter, d_f/μm	Fiber emissivity, e	Fiber density, ρ_f/g/cm^3	Fiber heat conductivity, k_s/w/m/k	Thickness, L_0/mm	Area density, μ/g/m^2	Porosity, ε
1	PET-100%	10.6	0.8	1.38	0.14	0.449	34	0.945
2	PET/VS-30/70	10	0.8	1.478	0.092	0.49	42.46	0.941
3	PET/VS-70/30	11.5	0.8	1.422	0.116	0.633	65.7	0.927
4	PET/VS-70/30	11.5	0.8	1.422	0.116	0.817	84.5	0.927
5	PP	21	0.97	0.91	0.12	0.317	44.5	0.845
6	PP	21	0.97	0.91	0.12	0.464	67.4	0.840
7	PP	21	0.97	0.91	0.12	0.63	101.3	0.809
8	PET/VS-20/80	15.5	0.8	1.49	0.086	0.615	141	0.846
9	Basalt	9	0.7	2.8	0.034	3.25	581	0.936

surfaces, and cubes can be described by Euclidean geometry using integer dimension 0, 1, 2, and 3, respectively. However, it is found that numerous objects in nature, such as rough surfaces, coastlines, mountains, rivers, lakes, and islands, are disordered and irregular, and they cannot be described by the Euclidean geometry because of the scale-dependent measures of length, area, and volume. These objects are called fractals, and the dimensions of such objects are non-integral and defined as fractal dimensions. A fractal object measurement $M(L)$ is related to the length scale L by the following power form [38].

$$M(L) \sim L^{D_f}, \tag{3}$$

where the "$\sim$" should be read as "scale as," M can be the length of a line, the area of a surface, the volume of a cube, or the mass of an object, D_f is the fractal dimension of the object, $0 < D_f < 2$ in two dimensions. For real porous media, the size distribution of pores satisfies the fractal power law [29, 30],

$$N(L \geq p) = \left(\frac{p_{max}}{p}\right)^{D_f}, \tag{4}$$

where p, and p_{max} are the pore size, and maximum pore size, separately.

The number of pores within the infinitesimal range p to $p + dp$ by differentiating Eq. 4 with respect to p.

$$-dN = D_f p_{max}^{D_f} p^{-(1+D_f)} dp. \tag{5}$$

The total number of pores (N_t) can be obtained from Eq. 2 in diameter range from p_{min} to p_{max}:

$$N_t(L \geq p_{min}) = \left(\frac{p_{max}}{p_{min}}\right)^{D_f}. \tag{6}$$

Dividing Eq. 6 by Eq. 5, Eq. 7 is obtained:

$$\frac{-dN}{N} = D_f p_{min}^{D_f} p^{-(1+D_f)} dp = f(p)dp. \tag{7}$$

In the above equation, $f(p)$ is the probability density function and should satisfy the following relationship (5).

$$\int_0^{\infty} f(p)dp = \int_{p_{min}}^{p_{max}} f(p)dp = 1 - \left(\frac{p_{min}}{p_{max}}\right)^{D_f} \equiv 1. \tag{8}$$

It is obviously seen that Eq. 8 holds if Eq. 9 is satisfied.

$$\frac{p_{min}}{p_{max}} \cong 0. \tag{9}$$

That is to say $p_{min} \ll p_{max}$ in Eq. 9 must be satisfied for fractal analysis of porous media. In general, $p_{min}/p_{max} \leq 10^{-2}$ in porous media, so the fractal theory can be used to study the characters of porous media.

It is considered that a unit cell in the fibrous assemblies includes a bundle of tortuous capillary tubes with variable cross-sectional area. Let the diameter of a capillary in the fibrous assembly be p and its tortuous length along the flow direction be $L(p)$. Due to the tortuous nature of the capillary, $L(p) \geq L_0$, with L_0 being the representative length. The equation, $L(p) = L_0$, holds for a straight capillary. When heat flow through the pores of the fibrous assemblies, the capillaries may be tortuous. These tortuous capillaries can be described by fractal equation [30]:

$$\frac{L(p)}{L_0} = \left(\frac{L_0}{p}\right)^{D_t - 1}, \tag{10}$$

where D_t is the tortuosity fractal dimension, in the range of $1 \leq D_t \leq 2$, which represents the extent of convolutedness of capillary pathways for heat flow through a medium. The higher the value D_t, the higher tortuous capillary. For a straight capillary path, $D_t = 1$, and the limiting case of $D_t = 2$ corresponds to a highly tortuous line that fills a plane.

The fractal model for effective heat conductivity

Heat transfer through a fibrous material involves combined modes of heat transfer: solid conduction through fibers, air conduction and natural convection in the space between fibers, and radiation interchange through participating media. Natural convection heat transfer in fibrous materials with densities greater than 20 kg/m^3 is negligible [39]. According to Stark and Fricke [40], the total heat flux (q_{sa}) passing through a fibrous material is:

$$q_{total} = q_{sa} + q_r, \tag{11}$$

where q_{sa} is the heat flux by solid fibers and air, and q_r is the heat flux due to radiation.

Using Fourier's law $q = -\lambda$ grad T, the total effective heat conductivity:

$$k_{eff} = k_{sa} + k_r. \tag{12}$$

Therefore, derivation of the effective heat conductivity can be divided into two parts, which are the derivation of solid and air heat conductivity, and the derivation of radiative heat conductivity, respectively.

Heat conductivity by solid and air (k_{sa})

In general, numerous capillary channels both parallel (Part A) and perpendicular (Part B) to heat flow direction for real fibrous assemblies, shown in Fig. 1, so the heat conductivity by solid and air can be divided into two parts, which are parallel and perpendicular heat conductivities k_{par} and k_{per}. The total heat conductivity by solid and air can be expressed as:

$$k_{sa} = \delta k_{per} + (1 - \delta) k_{par}, \tag{13}$$

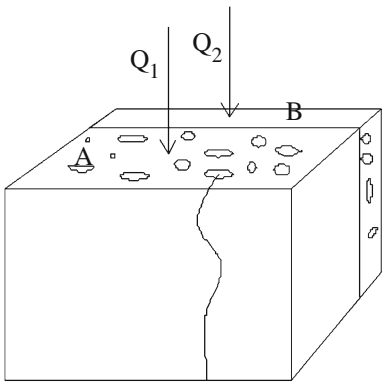

Fig. 1 Schematic diagram of fractal channel in fibrous material

where δ is the ratio of the number of perpendicular channels to the total number of channels, with values ranging from 0 to 1.

Fractal parallel model k_{par}

By heat-electric analogy approach, the parallel heat conductivity can be calculated by assuming that fibers and air channels are in parallel arrangement to heat flow.

According to the Fourier's law, the thermal resistance of a single channel r can be expressed as [41, 42]:

$$r(p) = \frac{L(p)}{Ak}, \tag{14}$$

where k is heat conductivity. The thermal resistance of a single air channel can be expressed as:

$$r_a(p) = \frac{L(p)}{A_a k_a} = \frac{4L(p)}{\pi p^2 k_a}. \tag{15}$$

The heat resistance of the air channels with the diameter between p and $p + dp$ can be written as:

$$R_{-dN}(p) = \frac{r_a(p)}{-dN} = \frac{4L(p)}{\pi p^2 k_a D_f p_{max}^{D_f} p^{-(D_f+1)} dp}. \tag{16}$$

Substituting Eq. 10 into Eq. 16, we can get Eq. 17.

$$R_{-dN}(p) = \frac{r_a(p)}{-dN} = \frac{4L_0^{D_t}}{\pi p^2 k_a D_f p_{max}^{D_f} p^{D_t - D_f} dp}. \tag{17}$$

According to heat-electrical analogy principle, the total heat resistance of air phase can be described as:

$$\begin{aligned} R_a(p) &= \frac{1}{\sum_{p_{min}}^{p_{max}} \frac{1}{R_{-dN}(p)}} = \frac{4L_0^{D_t}}{\sum_{p_{min}}^{p_{max}} \pi k_a D_f p_{max}^{D_f} p^{D_t - D_f} dp} \\ &= \frac{4L_0^{D_t}}{\int_{p_{min}}^{p_{max}} \pi k_a D_f p_{max}^{D_f} p^{D_t - D_f} dp} \\ &= \frac{4L_0^{D_t}(D_t - D_f + 1)}{\pi k_a D_f p_{max}^{D_t+1} \left[1 - \left(\frac{p_{min}}{p_{max}}\right)^{D_t - D_f + 1}\right]}. \end{aligned} \tag{18}$$

The heat transfer resistance caused by fibers can be written as:

$$R_s = \frac{L_0}{(1-\varepsilon)Ak_s}. \tag{19}$$

Theoretical modeling of solid conduction through fibers and points of contact between them is difficult, and various empirical relations have been developed to model the solid conduction. Model of Verschoor et al. [43] is used here, shown in Eq. 20,

$$k_s = (1-\varepsilon)^m k_s^*, \tag{20}$$

where m is the constant determined by comparing the experimental and theoretical results and k_s^* is the heat conductivity.

Therefore, the total parallel heat conductivity can be expressed as:

$$\begin{aligned} k_{par} &= \frac{L_0}{A}\left(\frac{1}{R_a} + \frac{1}{R_s}\right) \\ &= \frac{\pi D_f p_{max}^{D_t+1}\left[1 - \left(\frac{p_{min}}{p_{max}}\right)^{D_t - D_f + 1}\right]}{4A(D_t - D_f + 1)L_0^{D_t - 1}} k_a + (1-\varepsilon)k_s, \end{aligned} \tag{21}$$

where A is the surface area and can be expressed as:

$$\begin{aligned} A &= \frac{A_p}{\varepsilon} = -\frac{1}{\varepsilon}\int_{p_{min}}^{p_{max}} \frac{1}{4}\pi p^2 dN \\ &= \frac{1}{\varepsilon}\int_{p_{min}}^{p_{max}} \frac{1}{4}\pi p^2 D_f p_{max}^{D_f} p^{-(1+D_f)} dp \\ &= \frac{\pi D_f p_{max}^2}{4(2-D_f)\varepsilon}\left[1 - \left(\frac{p_{min}}{p_{max}}\right)^{2-D_f}\right]. \end{aligned} \tag{22}$$

Therefore, the total parallel heat conductivity can be obtained:

$$\begin{aligned} k_{par} &= \frac{L_0}{A}\left(\frac{1}{R_a} + \frac{1}{R_s}\right) \\ &= \frac{(2-D_f)\varepsilon\left[1 - \left(\frac{p_{min}}{p_{max}}\right)^{D_t - D_f + 1}\right]}{(D_t - D_f + 1)\left[1 - \left(\frac{p_{min}}{p_{max}}\right)^{2-D_f}\right]}\left(\frac{p_{max}}{L_0}\right)^{D_t - 1} k_a + (1 \\ &\quad - \varepsilon)k_s. \end{aligned} \tag{23}$$

Fractal perpendicular model

The perpendicular heat conductivity can be calculated by assuming that fibers and air channels are in perpendicular arrangement to heat flow. The perpendicular heat conductivity can be written as:

$$k_{per} = \frac{1}{\frac{\varepsilon}{k_a} + \frac{1-\varepsilon}{k_s}}. \tag{24}$$

Inserting Eqs. 23 and 24 into Eq. 13, we can get:

$$k_{sa} = (1-\delta) \times \left\{ \frac{(2-D_f)\varepsilon\left[1-\left(\frac{p_{min}}{p_{max}}\right)^{D_t-D_f+1}\right]}{(D_t-D_f+1)\left[1-\left(\frac{p_{min}}{p_{max}}\right)^{2-D_f}\right]}\left(\frac{p_{max}}{L_0}\right)^{D_t-1} k_a + (1-\varepsilon)k_s \right\} + \delta\frac{1}{\frac{\varepsilon}{k_a}+\frac{1-\varepsilon}{k_s}}. \quad (25)$$

Radiative heat conductivity k_r

The radiative heat conductivity can be obtained from the following equation, according to the studies by previous researchers [44–46].

$$k_r = C\sigma T^3 \frac{R'}{e(1-\varepsilon)}, \quad (26)$$

where R' is the radius of fiber, e is the emissivity of the fiber, σ is the Boltzmann constant, T is the temperature, and C is the constant determined by fiber orientation.

In the previous study, we got the new constant by comparing theoretical model and experiment results, which is more accurate [46].

$$k_r = 3.315\sigma T^3 \frac{R'}{e(1-\varepsilon)}. \quad (27)$$

The effective heat conductivity

The total effective heat conductivity can be obtained by substituting Eqs. 26 and 27 into Eq. 11.

$$k_{eff} = (1-\delta) \times \left\{ \frac{(2-D_f)\varepsilon\left[1-\left(\frac{p_{min}}{p_{max}}\right)^{D_t-D_f+1}\right]}{(D_t-D_f+1)\left[1-\left(\frac{p_{min}}{p_{max}}\right)^{2-D_f}\right]}\left(\frac{p_{max}}{L_0}\right)^{D_t-1} k_a + (1-\varepsilon)k_s \right\} + \delta\frac{1}{\frac{\varepsilon}{k_a}+\frac{1-\varepsilon}{k_s}} + 3.315\sigma T^3 \frac{R'}{e(1-\varepsilon)}. \quad (28)$$

There is no empirical parameter and every parameter has a clear physical meaning. Several parameters have to be determined in this equation, the pore area fraction D_f, the tortuosity fractal dimension D_t, the maximum pore size p_{max}, and the minimum pore size. The parameters were discussed in the following part.

Parameter determination

Pore area fractal dimension D_f

The pore area fractal dimension D_f is a parameter for characterizing the complex structure of porous media. It

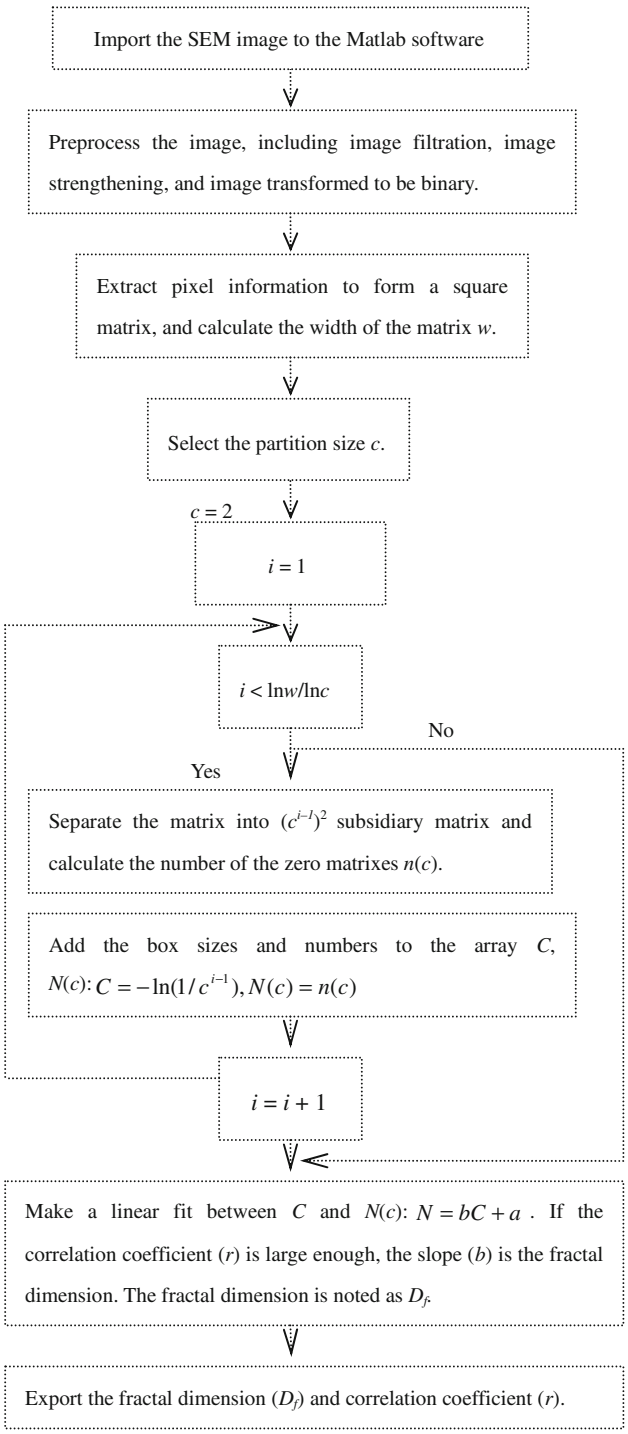

Fig. 2 Flow chart of determination pore area fractal dimension

can be obtained based on the box-counting method [13, 30]. This method is on the basis of the image analysis of a unit cell. The flow chart is shown in Fig. 2. The image processing analysis to the influence of the fractal dimension was investigated systematically by Tang et al. [16]. Image magnification was discovered to have little effect on the fractal dimension; on the contrary, threshold value is regarded to have obvious affect on the fractal dimension. Iteration method [47] was applied to get the best threshold value here. In the calculating step, the surface section under consideration is covered using square boxes of size (c, then the number of boxes ($N(c)$), required to completely cover the pore areas is counted. The pore area fractal dimension (D_f) can be determined by the value of the slope of a linear fit through data on a logarithmic plot of the cumulative number of pores $N(c)$ versus the pore size c.

Tortuosity fractal dimension

The determination of tortuosity fractal dimension can be classified into two categories. One is the box-counting method, which was proved successful in [14, 48]. The other is the analytical method, and several researchers have applied the method [49, 50]. Since it is complicated to get the cross-sectional area, parallel to the air flow, of the fibrous assemblies, the second method is applied.

As a matter of fact, Eq. 10 can be rewritten as:

$$\tau = \frac{L(p)}{L_0} = \left(\frac{L_0}{p}\right)^{D_t-1}. \tag{29}$$

The average tortuosity (τ_m) can be determined by substituting the average pore diameter (p_m) into Eq. 29.

$$D_t = 1 + \frac{\ln \tau_m}{\ln \frac{L_0}{p_m}}. \tag{30}$$

Then, the fractal dimension, D_t, for tortuous flow streamtubes in porous media can be obtained from Eq. 30 as:

$$\tau_m = \left(\frac{L_0}{p_m}\right)^{D_t-1}. \tag{31}$$

In the above equation, the average pore diameter p_m can be determined by Eq. 32.

$$\begin{aligned} p_m &= \int_{p_{\min}}^{p_{\max}} p f(p) \mathrm{d}p = \int_{p_{\min}}^{p_{\max}} p D_f p_{\min}^{D_f} p^{-(1+D_f)} \mathrm{d}p \\ &= \frac{D_f}{D_f - 1} p_{\min} \left[1 - \left(\frac{p_{\min}}{p_{\max}}\right)^{D_f-1}\right]. \end{aligned} \tag{32}$$

The tortuosity of fibrous materials was studied by some researchers [51–53]. The tortuosity model of fibrous assemblies developed by Koponen [52] is selected for calculation here, as it was proved to be more accurate.

$$\tau = 1 + 0.65 \frac{(1-\varepsilon)}{(\varepsilon - 0.33)^{0.19}}. \tag{33}$$

Accordingly, the tortuosity fractal dimension can be derived by substituting Eqs. 32 and 33 into Eq. 30.

$$D_t = 1 + \frac{\ln \tau_m}{\ln \frac{L_0}{p_m}} = 1 + \frac{\ln\left[1 + 0.65 \frac{(1-\varepsilon)}{(\varepsilon-0.33)^{0.19}}\right]}{\ln \frac{L_0(D_f-1)}{D_f p_{\min}\left[1-\left(\frac{p_{\min}}{p_{\max}}\right)^{D_f-1}\right]}}. \tag{34}$$

p_{max}, p_{min} determination

The biggest pore size $p_{\max}$ in fibrous assemblies has been discussed in series of papers [54, 55]. The expression can be expressed as:

$$p_{\max} = \frac{2.549}{\omega}, \tag{35}$$

where

$$\omega = \frac{8\mu}{\pi L_0 d_f \rho_f},$$

where ω is the total length of fibers per unit area, d_f is the fiber diameter, μ is the mass per unit area, and ρ_f is the density of fiber.

The minimum pore size $p_{\min}$ in fibrous assemblies has not been found in previous studies, and it is assumed to be expressed in Eq. 31.

$$p_{\min} = \frac{\theta}{\omega}, \tag{36}$$

where θ is the constant determined by comparing the experimental and theoretical results.

Results and discussion

Parameters determination in the fractal model

Firstly, parameters in the fractal model have to be determined. Figure 3 exhibits the image of the nonwoven fabric 5, as an example, before and after processing. The image is with the magnification of 100, resolution of 254 DPI, and size of 1280 pixel × 960 pixel.

Figure 4 shows the logarithmic plots of the cumulative number of macro-pores versus pore sizes of the nonwoven fabric. It is obvious that the number of cumulative pores increases with the increase of the pore size. The data follow a linear relationship on the logarithmic scale, which confirms the statistical fractal nature of the microstructures of the nonwoven fabrics. The fractal dimension can be derived from the slopes of these straight lines.

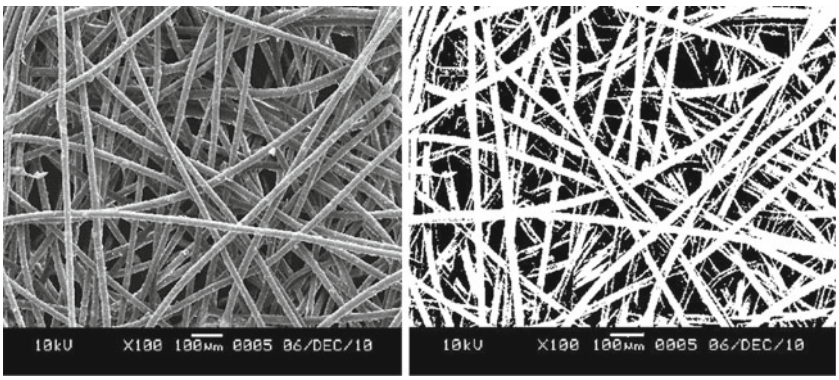

Fig. 3 SEM images of the nonwoven samples. **a** The SEM images before processing, **b** the binary images

The pore area fractal dimension D_f is calculated based on the images, and the maximum pore diameter p_{max} is derived by Eq. 36, listed in Table 2. The tortuosity fractal dimension D_t and the minimum pore diameter p_{min} are not shown in the table, as the two parameters are related to each other, which will be determined by comparing the experimental and fractal model predicting results of heat conductivity.

The effective heat conductivity determination by experiment

The experimental result is shown in Fig. 5. It can be seen from the figure that the effective heat conductivity decreases with the increase of porosity except the last two points. The testing temperature is 25 °C, and radiative heat conductivity is neglected. Heat conductivity by fibers and air is the main factor affecting the final effective heat conductivity. Sample 11 shows the lowest effective heat conductivity because of its super low fiber heat conductivity 0.034 W/m K. Samples 1 and 2 exhibit higher effective heat conductivity than sample 11 because of their higher fiber heat conductivity.

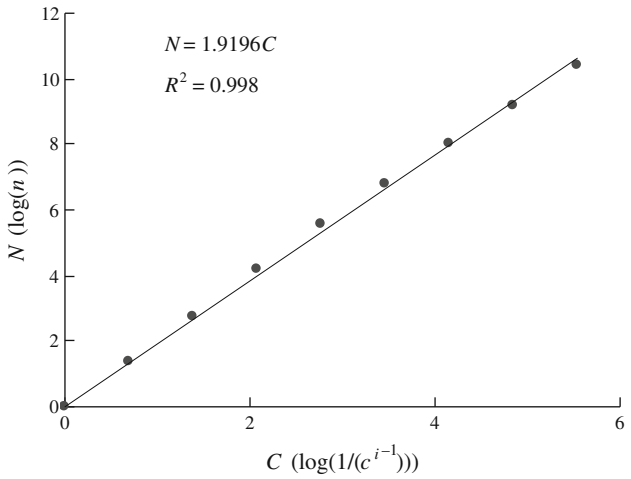

Fig. 4 The logarithmic plots of the cumulative number of pores versus pore sizes

Table 2 Parameters determined indirectly

Sample number	Pore area fractal dimension, D_f	The maximum pore diameter, p_{max}/μm
1.	1.9333	193.7
2.	1.9244	182.1
3.	1.9190	161.9
4.	1.9170	161.7
5.	1.9303	163.3
6.	1.9412	144.7
7.	1.9196	118.9
8.	1.9077	110.3
9.	1.8843	151.4

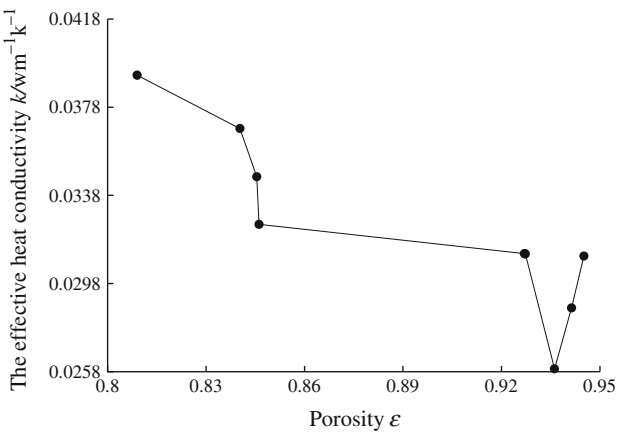

Fig. 5 The effective heat conductivity versus porosity by experiment

Comparison between fractal model and analysis models

Several representative analytical models developed by previous researchers are listed in Table 3. The fractal model is compared with the models.

Figure 6 shows the effective heat conductivities derived by the models and experiment. From the figure, it is found that the effective heat conductivities obtained by the

Table 3 Models of previous researchers

Reference	Heat conductivity equation	Specification
Hager and Steere [20]	$k = 4(1-\varepsilon)^m k_s + \frac{k_s k_g}{\varepsilon k_s + (1-\varepsilon)k_g}$	Hager and Steere used $m = 3$ to model the solid conduction in fibrous insulation and stated that it was an upper limiting value when contact with the fibers was less than perfect. For alumina fibrous insulation, $m = 1.4$ was determined using a parameter estimation technique in [17]. In the present investigation, $m = 3$ is used
Fanworth [25]	$k = \varepsilon k_a + (1-\varepsilon)k_f + \frac{8\sigma \overline{T}^3 R}{(1-\varepsilon)e}, \quad \overline{T} = \frac{T_1+T_2}{2}$	The model is valid for thick samples or those that are highly absorbing
Veiseh [28]	$\lambda(\rho,T) = 0.2572T_m^{0.81} + 0.0527\rho^{0.91}(1+0.0013T_m) + \frac{4\sigma T_m^3 L}{(\frac{2}{\varepsilon}-1)+0.001\overline{\beta}\rho L}$	The equation is obtained by combining Langlais and Klarsfeld semi-empirical relation for conduction heat transfer and Larkin formula for radiation part

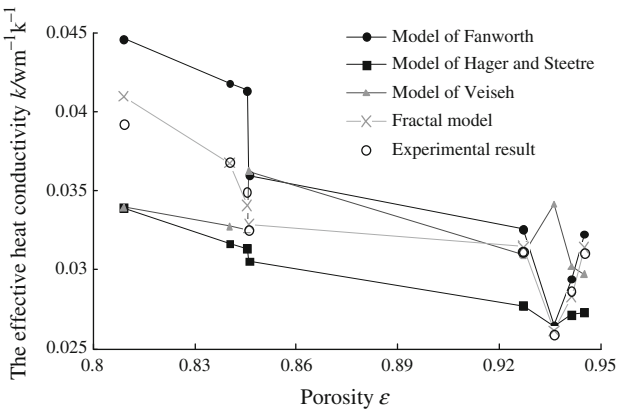

Fig. 6 The effective heat conductivity versus porosity of the models and experiment

models of Farnworth, Hager and Steetre, and fractal model here shows the same trend with the experimental result.

However, the model of Veiseh is the exception, indicating that the model is not validated. It is obvious to see that the effective heat conductivities obtained by the fractal model and experiment are in better accordance, showing the accuracy of the fractal model. The parameter m (indicating the effect of fiber-to-fiber contact to solid fiber conductivity) was calculated to be 0.05, which is similar to the result of Liu (0.058) [56]. θ was calculated to be 0.1 (the constant in the equation of the minimum pore diameter calculation). Using the result of θ, the minimum pore diameters of samples 2, 4, and 11 are calculated to be 7.5, 8.4, and 5.5 μm, respectively, very close to the results of the experiment done by Yang [57], which are 7.37, 8.27, and 5.32 μm.

Conclusions

In this article, fibrous materials were confirmed to have the fractal property by box-counting method.

A fractal model was developed for studying the effective heat conductivity of nonwoven fabrics. The fractal model indicates that the effective heat conductivity is related to the parameters, including the biggest and smallest pore diameter, the solid conductivity, the air conductivity, porosity, and temperature.

The theoretical results are compared with the experimental results and the previous formulas, from which the fractal model is confirmed, consequently, the parameter m, contained in the fiber-to-fiber contact influence on the effective heat conductivity equation, is confirmed to be 0.05 and the parameter θ, the coefficient in the minimum pore diameter equation, is determined to be 0.1.

Acknowledgements The authors thank Donghua University for the financial support under contract no. 10D10115.

References

1. Bankvail C. Heat transfer in fibrous materials. J Test Eval. 1973;3:235–43.
2. Egyed O, Simon J. Investigations on the flame-retardation of cellulosic fibrous materials. J Therm Anal Calorim. 1979;16:307–20.
3. Monald JM, George Lamb ER. Measurement of thermal conductivity of nonwovens using a dynamic method. Text Res J. 1987;57:721–7.
4. Mohammadi M, Banks LP, Ghadimi P. Determining effective thermal conductivity of multilayered nonwoven fabrics. Text Res J. 2003;73:802–8.
5. Mazzuchettl G, Lopardo G, Demichelis R. Influence of nonwoven fabrics' physical parameters on thermal and water vapor resistance. J Ind Text. 2007;36:253–64.
6. Chen JJ, Yu WD. A numerical analysis of heat transfer in an evacuated flexible multilayer insulation material. J Therm Anal Calorim. 2010;101:1183–8.
7. Hao LC, Yu WD. Evaluation of thermal protective performance of basalt fiber nonwoven fabrics. J Therm Anal Calorim. 2010;100:551–5.
8. Oldich J, Pan N. Thermo-insulating properties of perpendicular-laid versus cross-laid lofty nonwoven fabrics. Text Res J. 2000;70:121–8.
9. Du N, Fan JT, Wu HJ. Optimum porosity of fibrous porous materials for thermal insulation. Fiber Polym. 2008;9:27–33.

10. Wilson CA, Niven BE, Laing RM. Estimating thermal resistance of the bedding assembly from thickness of materials. Int J Cloth Sci Technol. 1999;11:262–76.
11. Yu BM, Cheng P. Fractal analysis of permeabilities for porous media. AIChE J. 2004;50:46–57.
12. Meng FG, Zhang HM, Li YS, Zhang XW, Yang FL, Xiao JN. Cake layer morphology in microfiltration of activated sludge wastewater based on fractal analysis. Sep Purif Technol. 2005;44:250–7.
13. Ozao R, Ochiai M. Fractal nature and thermal analysis of powders. J Therm Anal Calorim. 1993;104:61–7.
14. He GL, Zhao ZC, Ming PW, Abuliti A, Yin CY. A fractal model for predicting permeability and liquid water relative permeability in the gas diffusion layer of PEMFCs. J Power Sources. 2007;163:846–52.
15. Yang XH, Li DG. Quantitative expression of nonwovens' pore structure. Ind Text. 2005;1:10–5.
16. Tang HP, Zhu JL, Xi ZP, Di XB, Wang JY, Ao QB. Impact factors of fractal analysis of porous structure. Sci China Technol Sci. 2010;53:348–51.
17. Yang S, Yu WD, Pan N. Fractal approach to sound absorption behavior in cashmere fiber assembly. In: Proceedings of the 12th international wool research conference, vol 2; 2010, p. 827–831.
18. Schuhmeister J. Versuche uber das Warmeleitungsvermogen der Baumwolle, Schafwolle u Seide, Ber. K. Aka. Wien. Math.-Naturwiss. Klass. 1877;76:283.
19. Baxter S. Thermal conductivity of textiles. Pro Phys Soc Lond. 1945;58:105–18.
20. Hager NE, Steere RC Jr. Radiant heat transfer in fibrous thermal insulation. J Appl Phys. 1967;38:4663–8.
21. Tong TW, Yang QS, Tien CL. Radiative heat transfer in fibrous insulations-part II: experimental analytic study. J Heat Transf. 1983;105:76–81.
22. Lee SC, Cunnington GR. Conduction and radiation heat transfer in high porosity fiber thermal insulation. J Thermophys Heat Transf. 2000;14:121–36.
23. Daryabeigi K. Heat transfer in high temperature fibrous insulation. J Thermophys Heat Transf. 2003;17:10–20.
24. Zhao SY, Zhang BM, He XD. Temperature and pressure dependent effective thermal conductivity of fibrous insulation. Int J Heat Mass Transf. 2009;48:440–8.
25. Fanworth B. Mechanisms of heat flow through clothing insulation. Text Res J. 1983;53:717–25.
26. Fan JT, Luo ZG, Li Y. Heat and moisture transfer with sorption and condensation in porous clothing assemblies and numerical simulation. Int J Therm Sci. 2000;43:2989–3000.
27. Cheng XY, Fan JT. Simulation of heat and moisture transfer with phase change and mobile condensates in fibrous insulation. Int J Therm Sci. 2004;43:665–76.
28. Veiseh S, Khodabandeh N, Hakkaki-Fard A. Mathematical methods for heat conductivity relationship in fibrous heat insulations for practical applications. Asian J Civil Eng (Build Hous). 2009;10:201–14.
29. Yu BM, Lee LJ, Cao HQ. A fractal in-plane permeability model for fabrics. Polym Compos. 2002;23:201–21.
30. Yu BM, Cheng P. A fractal permeability model for bi-dispersed porous media. Int J Heat Mass Transf. 2002;45:2983–93.
31. Chen YP, Shi MH. Study on effective thermal conductivity of real porous media by using fractal theory. J Appl Sci. 2000;3:263–6.
32. Yu BM. Analysis of heat and mass transfer in fractal media. Int J Heat Mass Transf. 2003;3:481–3.
33. Yu ZT, Hu YC, Tian T, Fan LW. Fractal model for predicting effective thermal conductivity perpendicular to fibers of wood. J Zhejiang Univ. 2007;2:352–5.
34. Shi MH, Li XC, Chen YP. Determinating effective heat conductivity of polyurethane foam by fractal method. Sci China Ser E. 2006;36:560–8.
35. Gao J, Pan N, Yu WD. A fractal approach to goose down structure. Int J Nonlinear Sci Num. 2006;7:113–6.
36. Zhu FL, Zhang WY. Fractal model for effective thermal conductivity of emergency thermal protective fabrics. J Text Res. 2008;29:39–43.
37. Kou JL, Wu FM, Lu HG, Xu YS, Song FQ. The effective thermal conductivity of porous media on statistical self-similarity. Phys Lett A. 2009;374:62–5.
38. Mandelbrot BB. The fractal geometry of nature. New York: W.H. Freeman and Company; 1982.
39. Bhattacharyya RK. Heat transfer model for fibrous insulations, thermal insulation performance. American Society for Testing and Materials; 1980.
40. Stark C, Fricke J. Improved heat transfer models for fibrous insulations. Int J Heat Mass Transf. 1993;36:617–25.
41. Gebhart B. Heat conduction and mass diffusion. New York: McGraw-Hill; 1993.
42. Cussler EL. Diffusion-mass transfer in fluid systems. Cambridge: Cambridge University Press; 2000.
43. Verschoor JD, Greebler P, Manville NJ. Heat transfer by gas conduction and radiation in fibrous insulation. J Heat Transf. 1952;74:961–8.
44. Strong HM, Bundy FP, Bovenkerk HP. Flat panel vacuum thermal insulation. J Appl Phys. 1960;31:39–50.
45. Davis LB, Birkebak RC. On the transfer of energy in layers of fur. Biophys J. 1974;14:249–68.
46. Song WF, Yu WD. Study on radiative heat transfer property of fiber assemblies using FTIR. J Therm Anal Calorim. 2010;3:785–90.
47. Yin DF, Li YM, Wang YM, Wang L. Study on threshold selection method for images. J Comput Sci. 2008;3:136–8.
48. Zhang LZ. A fractal model for gas permeation through porous membranes. Int J Heat Mass Transf. 2008;51:5288–95.
49. Xu P, Yu BM. Developing a new form of permeability and Kozeny–Carman constant for homogeneous porous media by means of fractal geometry. Adv Water Resour. 2008;31:74–81.
50. Yu BM. Analysis of flow in fractal porous media. Appl Mech Rev. 2008;61:1–19.
51. Mohammadi M, Lee PB. Air permeability of multilayer needle punched nonwoven fabrics: theoretical method. J Ind Text. 2002;32:45–57.
52. Koponen A, Kandhai D, Helen E, Alava M, Hoekstra A, Kataja M, Niskanen K. Permeability of three-dimensional random fiber webs. Phys Rev Lett. 1998;80:716–9.
53. Vallabh R, Lee PB, Seyam AF. New approach for determining tortuosity in fibrous porous media. J Eng Fibers Polym. 2010;5:7–15.
54. Gérard L, André R, Claude W. Theoretical and experimental opening sizes of heat-bonded geotextiles. Text Res J. 1989;59:208–17.
55. Liu LF, Wang WZ, Chu CY, Chi JK. Study on relation between pore size distribution and permeability of nonwoven geotextile. J Qingdao Univ. 2002;1:1–5.
56. Liu RT. Study on heat transfer of disordered fiber assembly. J Text Res. 1995;5:265–7.
57. Yang S, Yu WD. Study on texture character and acoustic absorbent behavior of nonwovens. Tech Text. 2010;7:6–11.